Alkynethiolato and Alkyneselenolato Ruthenium Half-Sandwich Complexes: Synthesis, Structures, and Reactions with $(\eta^5\text{-}C_5H_5)_2Zr$

Yusuke Sunada,[†] Yuji Hayashi,[†] Hiroyuki Kawaguchi,[‡] and Kazuyuki Tatsumi*[,†]

Research Center for Materials Science, and Department of Chemistry, Graduate School of Science, Nagoya University, Furo-cho, Chikusa-ku, Nagoya 464-8602, Japan, and Coordination Chemistry Laboratories, Institute for Molecular Science, Myodaiji, Okazaki 444-8595, Japan

Received August 2, 2001

Alkynethiolato and alkyneselenolato complexes of ruthenium, $CpRu(PPh_3)_2(EC{\equiv}CR)$ ($Cp = \eta^5\text{-}C_5H_5$; E = S, R = Ph (**1a**), $SiMe_3$ (**1b**), ^{t}Bu (**1c**); E = Se, R = Ph (**2a**), $SiMe_3$ (**2b**)), were synthesized by the reactions of $CpRuCl(PPh_3)_2$ with corresponding lithium alkynechalcogenolates in THF. An analogous reaction of $Cp^*RuCl(PEt_3)_2$ ($Cp^* = \eta^5\text{-}C_5Me_5$) with LiSC≡CPh produced $Cp^*Ru(PEt_3)_2(SC{\equiv}CPh)$ (**3**). Complexes **1a** and **2a** were allowed to react in THF with "Cp_2Zr", generated in situ from Cp_2ZrCl_2 and 2 equiv of *n*-BuLi, from which the S-bridged Ru−Zr dinuclear complexes $CpRu(PPh_3)(C{\equiv}CPh)(\mu\text{-}S)ZrCp_2$ (**4a**) and $CpRu(PPh_3)(C{\equiv}CPh)(\mu\text{-}Se)ZrCp_2$ (**4b**) were isolated, respectively. In these complexes, C−S(Se) bond cleavage of the alkynechalcogenolate ligands was promoted by "Cp_2Zr", and the Zr atom was oxidized from II to IV. Treatment of **4a** and **4b** in THF under 1 atm CO gave rise to $CpRu(CO)(C{\equiv}CPh)(\mu\text{-}E)ZrCp_2$ (E = S (**5a**), Se (**5b**)), while addition of *tert*-butyl isocyanide to a THF solution of **4b** afforded $CpRu(CN^tBu)(C{\equiv}CPh)(\mu\text{-}Se)ZrCp_2$ (**6**). The crystal structures of **1a**, **1c**, **2a**, **2b**, **3**, **4a**, **4b**, and **5b** were determined by X-ray diffraction analysis.

Introduction

We recently began to investigate the chemistry of transition metal alkynethiolato and alkyneselenolato complexes.[1] Our interest in these complexes stem primarily from the two aspects. One is the unique ability of the ligands to be bound to a single- or multi-metal center at both chalcogen and alkyne portions, and a variety of unusual coordination geometries would be created. The other aspect is that having a reactive carbon−carbon triple bond adjacent to the chalcogen atom coordinated at a transition metal, new types of chemical transformations would be observed at the ligands. Previously, we reported syntheses and reactions of alkynethiolato and alkyneselenolato complexes of titanocene(IV) and samarocene(III). For example, the reaction of preformed $Cp_2Ti(SC{\equiv}CPh)_2$ with $Ni(\eta^4\text{-}C_8H_{12})_2$ gave rise to a trinuclear cluster $[Cp_2Ti(\mu\text{-}SC{\equiv}CPh)_2]_2Ni$ having a linear Ti_2Ni spine.[1] Independent from us, Delgado and Lalinde reported the synthesis of $(C_5H_4R')(C_5H_4SiMe_3)Ti(SC{\equiv}CR)_2$ (R = ^{t}Bu, Ph; R′ = $SiMe_3$, PPh_2), and the reactions with $Mo(CO)_3(CH_3CN)_3$, $Mo(CO)_4$(nbd), and $M(C_6F_5)_2(thf)_2$ (M = Pd, Pt) to afford $(C_5H_4SiMe_3)_2Ti(\mu\text{-}SC{\equiv}CR)_2ML_n$ (ML_n = $Mo(CO)_4$, $Pd(C_6F_5)_2$, $Pt(C_6F_5)_2$) and $(C_5H_4SiMe_3)Ti(\mu\text{-}\eta^5{:}\kappa\text{-}P\text{-}C_5H_4PPh_2)(SC{\equiv}C^tBu)(\mu\text{-}SC{\equiv}C^tBu)ML_n$ (ML_n = $Mo(CO)_3$, $Pd(C_6F_5)_2$, $Pt(C_6F_5)_2$).[2] In these dinuclear structures, two metal atoms are bridged by thiolato sulfurs, and the alkyne portion remains intact.

To develop the chemistry of heterobimetallic alkynechalcogenolato complexes, we planned to combine late transition metal complexes of alkynechalcogenolates and a reactive early transition metal fragment, viz zirconocene(II) generated in situ.[3−6] Zirconocene(II), Cp_2Zr, is known to activate alkynes and alkenes, affording various metallacycles via C−C bond forming reactions.[4] The reaction between $Cp_2Zr(CO)_2$ and R_2S_2 has been employed in the synthesis of thiolato complexes, $Cp_2Zr(SR)_2$ (R = Ph, Et),[5] and $[Cp_2Zr(\mu\text{-}E)]_2$ (E = S, Se) were prepared by the reaction between Cp_2Zr and elemental sulfur or selenium.[6] Thus, we report in this paper the preparation of a series of ruthenium(II) alkynechalcogenolato complexes, $CpRu(PPh_3)_2(EC{\equiv}CR)$ (E = S, R = Ph (**1a**), $SiMe_3$ (**1b**), ^{t}Bu (**1c**); E = Se, R = Ph (**2a**), $SiMe_3$ (**2b**)) and $Cp^*Ru(PEt_3)_2(SC{\equiv}CPh)$ (**3**). The reactions of $CpRu(PR_3)_2Cl$ with LiSC≡CR′ were reported to generate η^1-(*S*)-alkynethiolate complexes (R = Ph; R′ = Ph, $SiMe_3$) and an η^1-(*C*)-thioketenyl complex (R = Me; R′ = Ph); their X-ray structures have not been determined.[7] We also report

* To whom correspondence should be addressed. E-mail: i45100a@nucc.cc.nagoya-u.ac.jp. Fax: +81-52-789-2943.

[†] Nagoya University.

[‡] Institute for Molecular Science.

(1) Sugiyama, H.; Hayashi, Y.; Kawaguchi, H.; Tatsumi, K. *Inorg. Chem.* **1998**, *17*, 6773−6779.

(2) Ara, I.; Delgado, E.; Forniés, J.; Hernández, E.; Lalinde, E.; Mansilla, N.; Moreno, M. T. *J. Chem. Soc., Dalton Trans.* **1998**, 3199−3208.

(3) (a) Peulecke, N.; Ohff, A.; Tillack, A.; Baumann, W.; Kempe, R.; Burlakov, V. V.; Rosenthal, U. *Organometallics* **1996**, *15*, 1340−1344. (b) Baranger, A. M.: Bergman, R, G. *J. Am. Chem. Soc.* **1994**, *116*, 3822−3835.

(4) (a) Negishi, E.; Kondakov, D, Y.; Choueiry, D.; Kasai, K.; Takahashi, T. *J. Am. Chem. Soc.* **1996**, *118*, 9577−9588. (b) Rosenthal, U.; Ohff, A.; Baumann, W.; Kempe, R.; Tillack, A.; Burlakov, V. V. *Angew. Chem., Int, Ed. Engl.* **1994**, *33*, 1605−1607. (c) Pellny, P.-M.; Burlakov, V. V.; Baumann, W.; Spannenberg, A.; Kempe, R.; Rosenthal, U. *Organometallics* **1999**, *18*, 2906−2909. (d) Kemp, M. I.; Whitby, R. J.; Coote, S. J. *Synthesis* **1998**, 552−556. (e) Takahashi, T.; Xi, Z.; Obora, Y.; Suzuki, N. *J. Am. Chem. Soc.* **1995**, *117*, 2665−2666. (f) Jemmis, E. D.; Giju, K. T.; *J. Am. Chem. Soc.* **1998**, *120*, 6952−6964.

(5) Fochi, G.; Guidi, G.; Floriani, C. *J. Chem. Soc., Dalton Trans.* **1984**, 1253−1256.

(6) (a) Erker, G.; Mühlenbernd, T.; Benn, R.; Rufinska, A.; Tainturier, B.; Gautheron, B. *Organometallics* **1986**, *5*, 1620−1625. (b) Erker, G.; Mühlenbernd, T.; Nolte, R.; Petersen, J. L.; Tainturier, B.; Gautheron, B. *J. Organomet. Chem.* **1986**, *314*, C21 −C24.

(7) (a) Weigand, W. *Z. Naturforsch., Teil B* **1991**, *46*, 1333−1337. (b) Weigand, W.; Robl, C. *Chem. Ber.* **1993**, *126*, 1807−1809. (c) Weigand, W.; Weishäupl, M.; Robl, C. *Z. Naturforsch., Teil B* **1996**, *51*, 501−505.

10.1021/ic010826h CCC: $20.00
Published on Web 11/14/2001

the reactions of **1a** and **2a** with Cp_2Zr, which generated the intriguing sulfido(selenido) bridged heterobimetallic complexes, $CpRu(PPh_3)(C{\equiv}CPh)(\mu\text{-}E)ZrCp_2$ (E = S (**4a**), Se (**4b**)). These heterobimetallic complexes were readily transformed into $CpRu(CO)(C{\equiv}CPh)(\mu\text{-}E)ZrCp_2$ (E = S (**5a**), Se (**5b**)) and $CpRu(CN^tBu)(C{\equiv}CPh)(\mu\text{-}Se)ZrCp_2$ (**6**) by treatment with CO and CN^tBu.

Experimental Section

General. All reactions and manipulations of air-sensitive compounds were performed under an inert atmosphere using standard Schlenk techniques. Solvents such as THF, toluene, diethyl ether, and hexane were distilled from sodium/benzophenone ketyl under N_2. Lithium alkynethiolates and alkyneselenolates,[1,8] $CpRuCl(PPh_3)_2$, $Cp^*RuCl(PEt_3)_2$, and Cp_2ZrCl_2,[9] were prepared according to the literature procedures.

NMR spectra were recorded on a Varian INOVA 500 spectrometer operating at 500 MHz for ^1H, at 202 MHz for ^{31}P, and at 96 MHz for ^{77}Se. ^1H NMR chemical shifts were quoted in ppm relative to the residual protons of deuterated solvents. $^{31}P\{^1H\}$ and ^{77}Se NMR chemical shifts were referenced to signals of external 85% H_3PO_4 and Me_2Se, respectively. IR spectra were recorded on a Perkin-Elmer 2000 FT−IR spectrometer. For UV−visible spectra, a JASCO V-500 spectrometer was used. Elemental analyses were performed on a LECO CHNS-932 microanalyzer.

Synthesis of $CpRu(PPh_3)_2(SC{\equiv}CPh)$ (1a). Addition of LiSC≡CPh (0.28 mmol) in THF (10 mL) to $CpRu(PPh_3)_2Cl$ (0.20 g, 0.28 mmol) in THF (30 mL) gave a dark red solution. The mixture was stirred overnight at room temperature, and the solvent was removed in vacuo. The residue was treated with toluene (50 mL) and centrifuged to remove LiCl. The toluene solution was evaporated to dryness. The resulting solid was dissolved in THF (5 mL) and layered with hexane (15 mL). By standing the solution at room temperature, **1a** was obtained as dark-red crystals in 67% yield. ^1H NMR (C_6D_6): δ 4.46 (s, 5H, C_5H_5), 6.95−7.04 (m, 19H, Ph), 7.1 (m, 2H, Ph), 7.5 (m, 12H, Ph), 7.6 (m, 2H, Ph). ^{13}C NMR (C_6D_6): δ 74.40 (s, S−C≡C_β), 85.85 (t, $^2J_{C-P}$ = 1.9 Hz, C_5H_5), 102.99 (t, $^3J_{C-P}$ = 3.9 Hz, S-C_α≡C), 125.53 (s, Ph), 128.91 (m, Ph), 129.78 (s, Ph), 132.39 (s, Ph), 132.85 (s, Ph), 132.93(s, Ph), 134.75-(m, Ph), 139.61(m, Ph). $^{31}P\{^1H\}$ NMR (C_6D_6): δ 42.1. IR (Nujol mull/KBr): 2110 (s, $\nu_{C\equiv C}$) cm^{-1}. UV−visible (λ_{max}, nm (ϵ, $M^{-1}cm^{-1}$), THF): 346 (15600). Anal. Calcd for $C_{49}H_{40}SP_2Ru$: C, 71.42; H, 4.89; S, 3.89. Found: C, 69.70; H, 5.04; S, 3.97.

Synthesis of $CpRu(PPh_3)_2(SC{\equiv}CSiMe_3)$ (1b). Reaction of $CpRuCl(PPh_3)_2$ (0.32 g, 0.44 mmol) and LiSC≡$CSiMe_3$ (0.44 mmol) in THF (30 mL) followed by a workup similar to that described above yielded dark-red crystals of **1b** (0.23 g, 64%). ^1H NMR (C_6D_6): δ 7.5 (m, 12H, Ph), 6.95−7.00 (m, 18H, Ph), 4.40 (s, 5H, C_5H_5), 0.44 (s, 9H, SiMe_3). $^{31}P\{^1H\}$ NMR (C_6D_6): δ 42.2. IR (Nujol mull, KBr): 2033 (s, $\nu_{C\equiv C}$) cm^{-1}. Anal. Calcd for $C_{46}H_{44}SP_2SiRu$: C, 67.37; H, 5.41; S, 3.91. Found: C, 67.83; H, 5.32; S, 3.84.

Synthesis of $CpRu(PPh_3)_2(SC{\equiv}C^tBu)$ (1c). Reaction of $CpRuCl(PPh_3)_2$ (0.25 g, 0.34 mmol) and LiSC≡C^{t}Bu (0.34 mmol) in THF (40 mL), and the subsequent workup similar to that used for isolation of **1a** and **1b**, provided **1c** as dark-red crystals (0.15 g, 56%). ^1H NMR (C_6D_6): δ 7.7 (m, 4H, Ph), 6.9 (m, 26H, Ph), 4.44 (s, 5H, C_5H_5), 1.48 (s, 9H, CMe_3). $^{31}P\{^1H\}$ NMR (C_6D_6): δ 42.5. IR (Nujol mull, KBr): 2127 (s, $\nu_{C\equiv C}$) cm^{-1}. Anal. Calcd for $C_{47}H_{44}SP_2Ru$: C, 70.21; H, 5.52; S, 3.99. Found: C, 70.28; H, 4.84; S, 3.76.

Synthesis of $CpRu(PPh_3)_2(SeC{\equiv}CPh)$ (2a). Addition of a THF (0.6 mL) solution of LiSeC≡CPh (0.30 mmol) to $CpRuCl(PPh_3)_2$ (0.21 g, 0.29 mmol) in THF (40 mL) followed by a workup similar to that described above yielded dark-red crystals of **2a** (0.16 g, 64%). ^1H NMR ($CDCl_3$): δ 7.4 (m, 2H, Ph), 7.13−7.25 (m, 33H, Ph), 4.27 (s, 5H, C_5H_5). $^{31}P\{^1H\}$ NMR ($CDCl_3$): δ 42.5. ^{77}Se NMR ($CDCl_3$): δ −364 (t, $^2J_{Se-P}$ = 21.0 Hz). IR (Nujol mull, KBr): 2110 (s, $\nu_{C\equiv C}$) cm^{-1}. Anal. Calcd for $C_{49}H_{40}SeP_2Ru$: C, 67.58; H, 4.63. Found: C, 67.88; H, 4.84.

Synthesis of $CpRu(PPh_3)_2(SeC{\equiv}CSiMe_3)$ (2b). Again, the procedure used for the isolation of **1a** was applied to the synthesis of **2b**. Thus, reaction of LiSeC≡CSiMe3 (0.45 mmol) with $CpRuCl(PPh_3)_2$ (0.32 g, 0.45 mmol) in THF (40 mL) afforded 0.24 g of **2b** as dark-red crystals in 63% yield. ^1H NMR ($CDCl_3$): δ 7.16−7.28 (m, 30H, Ph), 4.22 (s, 5H, C_5H_5), 0.24 (s, 9H, SiMe_3). $^{31}P\{^1H\}$ NMR ($CDCl_3$): δ 42.7. ^{77}Se NMR ($CDCl_3$): δ −362 (t, $^2J_{Se-P}$ = 20.7 Hz). IR (Nujol mull, KBr): 2037 (s, $\nu_{C\equiv C}$) cm^{-1}. Anal. Calcd for $C_{46}H_{44}SiSeP_2Ru$: C, 63.72; H, 5.12. Found: C, 63.35; H, 5.10.

Synthesis of $Cp^*Ru(PEt_3)_2(SC{\equiv}CPh)$ (3). A mixture of $Cp^*RuCl(PEt_3)_2$ (0.20 g, 0.39 mmol) and LiSC≡CPh (0.39 mmol) in THF (40 mL) was treated as described for the synthesis of **1a**. The resulting residue was recrystallized from Et_2O to yield 0.23 g of **3** as orange crystals (68%). ^1H NMR (C_6D_6): δ 7.60 (m, 2H, Ph), 7.08 (m, 2H, Ph), 6.97 (m, 1H, Ph), 1.78−1.95 (m, 12H, PCH_2CH_3), 1.67 (s, 15H, C_5Me_5), 0.96−1.06 (m, 18H, PCH_2CH_3). $^{31}P\{^1H\}$ NMR (C_6D_6): δ 23.8. IR (Nujol mull, KBr): 2120 (s, $\nu_{C\equiv C}$) cm^{-1}. Anal. Calcd for $C_{30}H_{50}SP_2Ru$: C, 59.47; H, 8.32; S, 5.29. Found: C, 58.64; H, 8.59; S, 5.05.

Synthesis of $CpRu(PPh_3)(C{\equiv}CPh)(\mu{-}S)ZrCp_2$ (4a). To a solution of Cp_2ZrCl_2 (65.4 mg, 0.22 mmol) in 20 mL of THF was added 0.29 mL of a 1.57 M hexane solution of *n*-BuLi (0.44 mmol) at −78 °C. The solution turned yellow, to which **1a** (0.18 g, 0.22 mmol) in THF (20 mL) was immediately added at −78 °C. After warming the reaction mixture to room temperature, the solution was stirred for 1 day. The solvent was removed in vacuo, and the resulting solid was treated with toluene (20 mL). An insoluble material was removed by centrifugation, and the supernatant was evaporated to dryness. The residue was recrystallized from THF/hexane (5 mL, 15 mL) to give **4a** as red crystals (0.12 g, 70%). ^1H NMR (C_6D_6): δ 7.91−7.94 (m, 6H, Ph), 7.71 (m, 2H, Ph), 7.34 (m, 2H, Ph), 6.97−7.05 (m, 10H, Ph), 5.71 (s, 5H, Zr-(C_5H_5)), 5.23 (s, 5H, Zr(C_5H_5)), 4.67 (s, 5H, Ru(C_5H_5)). ^{13}C NMR (C_6D_6): δ 88.27 (d, $^2J_{C-P}$ = 2.9 Hz, Ru(C_5H_5)), 107.80 (s, Zr(C_5H_5)), 109.71 (s, Zr(C_5H_5)), 115.79 (s, Ru−C≡C_β), 126.38 (s, Ph), 129.32 (s, Ph), 129.87 (m, Ph), 131.87 (s, Ph), 135.67(m, Ph), 138.76(s, Ph), 139.10 (s, Ph), 188.65 (d, $^2J_{C-P}$ = 19.6 Hz, Ru-C_α≡C). IR (Nujol mull, KBr): 1926 (s, $\nu_{C\equiv C}$) cm^{-1}. Anal. Calcd for $C_{41}H_{35}SPRuZr\cdot 1/2THF$: C, 63.04; H, 4.80; S, 3.91. Found: C, 62.60; H, 5.11; S, 3.75.

Synthesis of $CpRu(PPh_3)(C{\equiv}CPh)(\mu{-}Se)ZrCp_2$ (4b). This compound was synthesized starting from Cp_2ZrCl_2 (0.038 g, 0.13 mmol), *n*-BuLi (1.54 M, 0.16 mL, 0.25 mmol), and **2a** (0.11 g, 0.13 mmol), according to the procedure described for the synthesis of **4a**. Compound **4b** was obtained as brown crystals (0.09 g) in 84% yield. ^1H NMR (C_6D_6): δ 7.90−7.94 (m, 6H, Ph), 7.72 (m, 2H, Ph), 7.36 (m, 2H, Ph), 7.18 (m, 1H, Ph), 6.98−7.04 (m, 9H, Ph), 5.66 (s, 5H, Zr(C_5H_5)), 5.18 (s, 5H, Zr(C_5H_5)), 4.66 (s, 5H, Ru(C_5H_5)). ^{13}C NMR (C_6D_6): δ 87.88 (d, $^2J_{C-P}$ = 2.9 Hz, Ru(C_5H_5)), 107.26(s, Zr(C_5H_5)), 109.10 (s, Zr-(C_5H_5)), 116.98 (s, Ru−C≡C_β), 126.14 (s, Ph), 129.34 (s, Ph), 129.84 (m, Ph), 131.78 (s, Ph), 135.77(m, Ph), 138.92(s, Ph), 139.26 (s, Ph), 193.68 (d, $^2J_{C-P}$ = 20.1 Hz, Ru-C_α≡C). $^{31}P\{^1H\}$ NMR (C_6D_6): δ 50.9 (s). ^{77}Se NMR (C_6D_6): δ 522 (br). IR (Nujol mull, KBr): 1920 (s, $\nu_{C\equiv C}$) cm^{-1}. Anal. Calcd for $C_{41}H_{35}SePRuZr$: C, 59.33; H, 4.25. Found: C, 59.91; H, 4.56.

Synthesis of $CpRu(CO)(C{\equiv}CPh)(\mu{-}S)ZrCp_2$ (5a). A THF (20 mL) solution of **4a** (0.20 g, 0.26 mmol) was stirred overnight under 1 atm of CO at room temperature. The solvent was removed in vacuo to leave an orange solid. Washing the solid with hexane (3 × 20 mL) gave 0.12 g of **5a** as an orange powder (83%). ^1H NMR (C_6D_6): δ 7.53 (m, 2H, Ph), 7.24 (m, 2H, Ph), 7.11 (m, 1H, Ph), 5.82 (s, 5H, Zr(C_5H_5)), 5.46 (s, 5H, Zr(C_5H_5)), 4.83 (s, 5H, Ru(C_5H_5)). IR (Nujol mull, KBr): 1965 (s, $\nu_{C\equiv O}$), 1926 (s, $\nu_{C\equiv C}$) cm^{-1}.

Synthesis of $CpRu(CO)(C{\equiv}CPh)(\mu{-}Se)ZrCp_2$ (5b). A THF (15 mL) solution of **4b** (0.11 g, 0.13 mmol) was treated under 1 atm of CO, as described for the synthesis of **5a**. The solution was concentrated to 2 mL in vacuo, and slow addition of hexane resulted in the depositing of **5b** as reddish brown crystals (0.05 g, 63%). ^1H NMR (C_6D_6): δ 7.53 (m, 2H, Ph), 7.20 (m, 2H, Ph), 7.13 (m, 1H, Ph), 5.76 (s, 5H,

(8) (a) Raap, R.; Micetich, R, G. *Can. J. Chem.* **1967**, *46*, 1057−1062. (b) M, Schmidt.; V, Potschka. *Naturwissenschaften* **1963**, *50*, 302.
(9) (a) Reid, A, F.; Wailes, P, C. *Aust. J. Chem.* **1966**, *19*, 309−312. (b) Bruce, M, I.; Windsor, N, J. *Aust. J. Chem.* **1977**, *30*, 1601−1604. (c) Coto, A.; Tenorio, M. J.; Puerta, M. C.; Valerga, P. *Organometallics* **1998**, *17*, 4392−4399.

Table 1. Crystal Data for $CpRu(PPh_3)_2(SC{\equiv}CPh)$ (**1a**), $CpRu(PPh_3)_2(SC{\equiv}C^tBu)$ (**1c**), $CpRu(PPh_3)_2(SeC{\equiv}CPh)$ (**2a**), $CpRu(PPh_3)_2(SeC{\equiv}CSiMe_3)$ (**2b**), $Cp^*Ru(PEt_3)_2(SC{\equiv}CPh)$ (**3**), $CpRu(PPh_3)(C{\equiv}CPh)(\mu\text{-}S)ZrCp_2$ (**4a**), $CpRu(PPh_3)(C{\equiv}CPh)(\mu\text{-}Se)ZrCp_2$ (**4b**), and $CpRu(CO)(C{\equiv}CPh)(\mu\text{-}Se)ZrCp_2$ (**5b**)

	1a	**1c**	**2a**	**2b**	**3**	**4a**	**4b**	**5b**
formula	$C_{49}H_{40}P_2SRu$	$C_{47}H_{44}P_2SRu$	$C_{52}H_{40}P_2SeRu$	$C_{46}H_{44}SiP_2SeRu$	$C_{30}H_{50}P_2SRu$	$C_{41}H_{35}PSZrRuC_4H_8O$	$C_{41}H_{35}PSeZrRuC_4H_8O$	C24H20OSeZrRu
mol wt (g mol^{-1})	823.93	803.94	906.87	866.92	605.80	831.14	902.06	895.67
cryst syst	monoclinic	triclinic	monoclinic	monoclinic	monoclinic	triclinic	triclinic	monoclinic
space group	$P2_1/n$ (No. 14)	P-1 (No. 2)	$P2_1/n$ (No. 14)	$P2_1/n$ (No. 14)	$P2_1/n$ (No. 14)	P-1 (No. 2)	P-1 (No. 2)	$P2_1/n$ (No. 14)
cryst color	dark red	dark red	dark red	dark red	orange	red	brown	reddish brown
cryst size	0.50 × 0.50 × 0.10	0.03 × 0.02 × 0.01	0.20 × 0.40 × 0.50	0.70 × 0.55 × 0.30	0.35 × 0.20 × 0.15	0.40 × 0.10 × 0.05	0.50 × 0.10 × 0.01	0.20 × 0.4 × 0.10
a (Å)	14.4564(7)	10.2855(8)	16.007(4)	15.959(5)	11.3623(3)	8.1073(6)	8.198(3)	16.400(5)
b (Å)	18.6851(3)	13.976(2)	15.255(3)	15.207(5)	14.1584(2)	13.635(1)	13.851(5)	8.240(3)
c (Å)	18.1251(2)	14.583(2)	18.023(4)	17.67(1)	18.4452(3)	18.153(1)	18.253(7)	16.908(4)
α (deg)	99.030(5)				111.9925(6)	112.416(3)		
β (deg)	105.5330(4)	108.290(2)	108.62(2)	105.94(4)	95.9407(8)	97.3595(8)	97.215(7)	113.93(2)
γ (deg)	100.284(2)				92.0565(9)	91.569(9)		
V (Å^3)	3959.8(2)	1906.8(3)	4170(1)	4123(2)	2951.38(9)	1837.7(2)	1894(1)	2088(1)
Z	4	2	4	4	4	2	2	4
ρ_{calc} (g cm^{-3})	1.382	1.400	1.444	1.396	1.363	1.545	1.581	1.894
μ (Mo Kα) (cm^{-1})	5.64	5.83	13.61	14.01	7.28	8.30	17.11	29.77
abs range	0.74−1.00	0.66−1.02	0.86−1.00	0.86−1.00	0.83−1.00	0.68−1.01	0.50−1.01	0.91−1.00
$2\theta_{max}$ (deg)	55	55	50	50	55	55	55	50
no. of meas rflns	23579	12987	7940	7856	19867	11922	11004	3824
no. of obs data[a]	8332	8724	4069	5625	5835	5169	3065	2422
no. param residuals	478	460	490	460	307	420	413	253
R^b	0.047	0.062	0.040	0.029	0.029	0.056	0.044	0.040
Rw^c	0.062	0.062	0.041	0.037	0.042	0.076	0.052	0.041
GOF[d]	3.30	1.28	1.33	1.68	2.37	2.08	1.58	1.64

[a] Observation criterion $I > 3\sigma(I)$. [b] $R = \sum||F_o| - |F_c||/\sum|F_o|$. [c] $Rw = [\{\sum w(|F_o| - |F_c|)^2\}/\sum wF_o^2]^{1/2}$. [d] $GOF = [\{\sum w(|F_o| - |F_c|)^2\}/(N_o - N_p)]^{1/2}$, where N_o and N_p denote the number of data and parameters.

$Zr(C_5H_5)$), 5.55 (s, 5H, $Zr(C_5H_5)$), 4.82 (s, 5H, $Ru(C_5H_5)$). ^{77}Se NMR (C_6D_6): δ 411(br). IR (Nujol mull, KBr): 1970 (s, $\nu_{C\equiv O}$), 1925 (s, $\nu_{C\equiv C}$) cm^{-1}. Anal. Calcd for $C_{18}H_{20}OSeRuZr$: C, 48.38; H, 3.38. Found: C, 48.72; H, 3.33.

Synthesis of $CpRu(CN^tBu)(C{\equiv}CPh)(\mu{-}Se)ZrCp_2$ (6). To a THF (5 mL) solution of **4b** (0.063 g, 0.076 mmol) was added ^{t}BuNC (8.5 μL, 0.076 mmol). After stirring the reaction mixture overnight at room temperature, the solution was concentrated to 2 mL. Addition of hexane led to the formation of **6** as reddish brown crystals (0.03 g, 62%). ^{1}H NMR (C_6D_6): δ 7.73 (m, 2H, Ph), 7.28 (m, 2H, Ph), 7.14 (m, 1H, Ph), 5.83 (s, 5H, $Zr(C_5H_5)$), 5.67 (s, 5H, $Zr(C_5H_5)$), 4.95 (s, 5H, $Ru(C_5H_5)$), 0.97 (s, 9H, CMe_3). IR (Nujol mull, KBr): 2120 (s, $\nu_{C\equiv N}$), 1910 (s, $\nu_{C\equiv C}$) cm^{-1}. Anal. Calcd for $C_{28}H_{29}NSeRuZr$: C, 51.67; H, 4.49; N, 2.15. Found: C, 51.01; H, 4.33; N, 1.86.

X-ray Crystal Structure Determination. Crystallographic data are summarized in Table 1. Crystals of **2a**, **2b**, and **5b** suitable for X-ray analysis were mounted in glass capillaries and sealed under argon. Diffraction data were collected at room temperature on a Rigaku AFC7R diffractometer, employing graphite-monochromated Mo Kα radiation (λ = 0.710 690 Å) and the $\omega - 2\theta$ scan technique. Refined cell dimensions and their standard deviations were obtained by least-squares refinements of 25 randomly selected centered reflections. Three standard reflections, monitored periodically for crystal decomposition or movement, did not show intensity decay over the course of the data collections. The raw intensities were corrected for Lorentz and polarization effects. Empirical absorption corrections based on ψ scans were successfully applied.

Crystals of **1a**, **1c**, **3**, **4a**, and **4b** were mounted on top of quartz fibers using perfluoro(polyoxypropylene ethyl ether) and were set on a Rigaku AFC7 equipped with a MSC/ADSC Quantum1 CCD detector. The measurements were made using Mo Kα radiation at −80 °C under a cold nitrogen stream. Four preliminary data frames were measured at 0.5 ° increments of ω, to assess the crystal quality, and preliminary unit cell parameters were calculated. The intensity images were measured at 0.5 ° intervals of ω for a duration of 35 s for **1a**, 152 s for **1c**, 35 s for **3**, 100 s for **4a**, and 35 s for **4b**. The frame data were integrated using a d*TREK program package, and the data sets were corrected for absorption using a REQAB program.

All calculations were performed with a TEXSAN program package. All structures were solved by direct methods, and then, the structures were refined by full-matrix least squares. Anisotropic refinement was applied to all non-hydrogen atoms, and all the hydrogen atoms were put at calculated positions. In the case of **4a** and **4b**, crystal solvents (THF) were defined as constrained groups. Additional information is available as Supporting Information.

Results and Discussion

Synthesis of Ruthenium(II) Alkynethiolato and Alkyneselenolato Complexes. The alkynechalcogenolato complexes, $CpRu(PPh_3)_2(EC{\equiv}CR)$ (E = S, R = Ph (**1a**), $SiMe_3$ (**1b**), ^{t}Bu (**1c**); E = Se, R = Ph (**2a**), $SiMe_3$ (**2b**)) and $Cp^*Ru(PEt_3)_2(SC{\equiv}CPh)$ (**3**), were prepared by the reactions of $CpRuCl(PPh_3)_2$ and $Cp^*RuCl(PEt_3)_2$ with 1 equiv of the corresponding lithium alkynechalcogenolates, respectively, Scheme 1. After standard workup, these complexes were isolated in 56−68% yields as dark-red crystals for **1a**, **b**, **c**, and **2a**, **b**, and as orange crystals for **3**. These alkynechalcogenolato complexes were characterized by elemental analysis, IR, and ^{1}H, ^{31}P{^{1}H}, and ^{77}Se NMR spectra.

The presence of S- or Se-coordinated alkynechalcogenolato ligands in **1**−**3** was indicated by strong IR bands in the 2037−2127 cm^{-1} region assignable to the C≡C stretching vibrational

Scheme 1

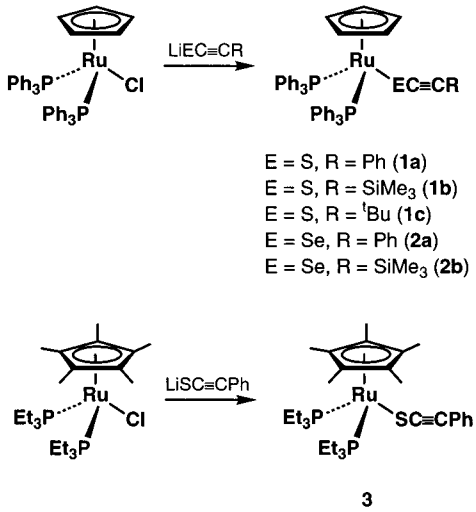

Table 2. Comparison of the C≡C Stretching Bands

complex	C≡C stretching band (cm^{-1})
$CpRu(PPh_3)_2(SC{\equiv}CPh)$ (**1a**)	2110
$CpRu(PPh_3)_2(SC{\equiv}CSiMe_3)$ (**1b**)	2033
$CpRu(PPh_3)_2(SC{\equiv}C^tBu)$ (**1c**)	2127
$CpRu(PPh_3)_2(SeC{\equiv}CPh)$ (**2a**)	2110
$CpRu(PPh_3)_2(SeC{\equiv}CSiMe_3)$ (**2b**)	2037
$Cp^*Ru(PEt_3)_2(SC{\equiv}CPh)$ (**3**)	2120
$CpRu(PPh_3)(C{\equiv}CPh)(\mu\text{-}S)ZrCp_2$ (**4a**)	1926
$CpRu(PPh_3)(C{\equiv}CPh)(\mu\text{-}Se)ZrCp_2$ (**4b**)	1920
$CpRu(CO)(C{\equiv}CPh)(\mu\text{-}S)ZrCp_2$ (**5a**)	1926
$CpRu(CO)(C{\equiv}CPh)(\mu\text{-}Se)ZrCp_2$ (**5b**)	1925
$CpRu(CN^tBu)(C{\equiv}CPh)(\mu\text{-}Se)ZrCp_2$ (**6**)	1910

mode. The $\nu_{C\equiv C}$ values of the coordinated alkynechalcogenolates vary notably depending on the R substituents; interestingly, choice of the chalcogen atom does not affect $\nu_{C\equiv C}$ very much, as shown in Table 2. Among the three substituents, trimethysilyl gives the lowest $\nu_{C\equiv C}$ value. The ^1H NMR data for **1**−**3** are consistent with their formulations, and each of the $^{31}P\{^1H\}$ NMR spectra exhibit a single resonance. In the ^{13}C NMR spectra of **1a**, the alkynyl α carbon resonance appears at 74.40 ppm with a coupling with the ^{31}P nuclei. In addition, the alkyneselenolato complexes of **2a** and **2b** were characterized by the triplet signals of ^{77}Se NMR at −364 ppm ($^2J_{Se-P}$ = 21.0 Hz) and −362 ppm ($^2J_{Se-P}$ = 20.7 Hz), respectively. These alkynethiolato and alkyneselenolato complexes are air- and moisture-sensitive, but are thermally robust. They show no sign of decomposition in boiling THF and toluene for 4 days under argon.

Crystals of **1a**, **1c**, **2a**, **2b**, and **3** were subject to X-ray crystallographic analysis. Because their molecular structures are very much alike, only the ORTEP views of **1a** and **3** are presented in Figures 1 and 2, respectively. Selected bond distances and angles of **1a**, **1c**, **2a**, **2b**, and **3** are summarized in Table 3. These complexes assume a common three-legged piano stool geometry with one chalcogen and two phosphorus atoms, and alkynethiolato and alkyneselenolato ligands coordinate at Ru from the S(Se) sites regardless of the substituents.

The Ru−S bond lengths of 2.4206(5)−2.4216(7) Å for **1a**, **1c**, and **3** are slightly shorter than those of the known Ru(II) thiolato complexes, e.g., $Ru(SC_6H_3Me_2\text{-}2,6)_2(CN^tBu)_4$ (av. 2.463 Å),[10] $Ru(SPh)_2(dmpe)_2$ (2.469 Å),[11] and $Ru(SC_6H_4Me\text{-}4)_2(CO)_2(PPh_3)_2$ (2.460 Å).[12] The Ru−Se bond distances of **2a** and **2b**

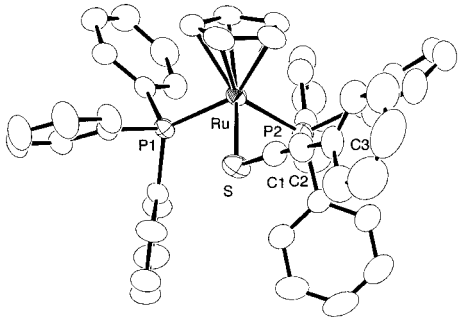

Figure 1. Structure of $CpRu(PPh_3)_2(SC{\equiv}CPh)$ (**1a**) showing 50% probablity ellipsoids.

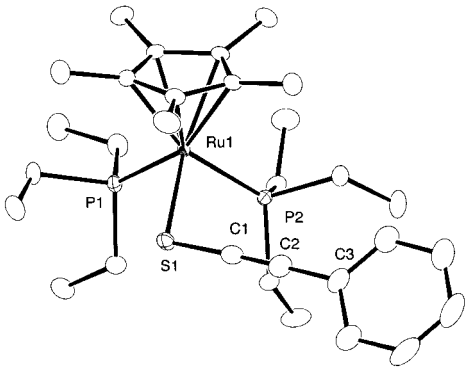

Figure 2. Structure of $Cp^*Ru(PEt_3)_2(SC{\equiv}CPh)$ (**3**) showing 50% probablity ellipsoids.

Table 3. Selected Bond Distances (Å) and Angles (deg) for $CpRu(PPh_3)_2(SC{\equiv}CPh)$ (**1a**), $CpRu(PPh_3)_2(SC{\equiv}C^tBu)$ (**1c**), $CpRu(PPh_3)_2(SeC{\equiv}CPh)$ (**2a**), $CpRu(PPh_3)_2(SeC{\equiv}CSiMe_3)$ (**2b**), and $Cp^*Ru(PEt3)2(SC{\equiv}CPh)$ (**3**)

	1a	**1c**	**2a**	**2b**	**3**
Ru−E	2.4216(7)	2.4207(9)	2.5469(8)	2.5390(5)	2.4206(5)
Ru−P1	2.3174(7)	2.3298(9)	2.317(2)	2.329(1)	2.3101(5)
Ru−P2	2.3440(8)	2.317(1)	2.326(2)	2.3284(9)	2.3242(6)
E−C1	1.668(3)	1.664(4)	1.828(7)	1.833(4)	1.676(2)
C1−C2 (C≡C)	1.207(5)	1.211(6)	1.196(9)	1.213(5)	1.214(3)
Ru−E−C1	109.5(1)	112.9(1)	102.2(2)	105.7(1)	105.21(8)
E−Ru−P1	89.49(2)	84.81(3)	93.28(4)	91.30(2)	89.83(2)
E−Ru−P2	90.15(3)	90.58(3)	89.70(5)	91.74(2)	90.12(2)
P1−Ru−P2	103.17(3)	103.37(3)	102.31(6)	102.04(3)	91.32(2)
E−C1−C2	175.5(3)	173.3(4)	178.3(7)	176.6(4)	178.1(2)
P1−Ru−E−C1	165.7(1)	165.3(2)	156.7(2)	91.9(1)	149.64(9)
P2−Ru−E−C2	91.1(1)	91.4(2)	101.0(2)	166.0(1)	58.33(9)

are 0.117−0.126 Å longer than the Ru−S bonds of **1a** and **1c**, which may reflect the increase in ionic radius from sulfur to selenium.[13] For **1a**, **1c**, **2a**, and **2b**, the alkyne groups bend up toward Cp, thus orienting away from the phosphine ligands in order to avoid steric congestion. On the other hand, the alkyne group of **3** lies between the PEt_3 and Cp* ligands, because the bulkiness of Cp* comes into play. The Ru−E−C1 angles fall in the normal range found in thiolato and selenolato complexes.[10−12,13b] The Ru−S−C1 angles of **1a** and **1c** are larger by 4−10° when compared with the Ru−Se−C1 angles of **2a** and **2b**, the trend of which is normal for chalcogenolato complexes.[1,14] The C≡C distances of **1a**, **1c**, **2a**, **2b**, and **3** are essentially the same irrespective of substituents, and they are

(10) Mashima, K.; Kaneyoshi, H.; Kaneko, S.; Mikami, A.; Tani, K.; Nakamura, A. *Organometallics* **1997**, *16*, 1016−1025.

(11) Field, L. D.; Hambley, T. W.; Yau, B. C. K. *Inorg. Chem.* **1994**, *33*, 2009−2017.

(12) Jessop, P. G.; Retting, S. J.; Lee, C. L.; James, B. R. *Inorg. Chem.* **1991**, *30*, 4617−4627.

(13) (a) Shannon, R. D. *Acta Crystallogr.* **1976**, *A32*, 751−767. (b) Millar, M. M.; O'Sullivan, T.; de Vries, N.; Koch, S. A. *J. Am. Chem. Soc.* **1985**, *107*, 3714−3715.

Scheme 2

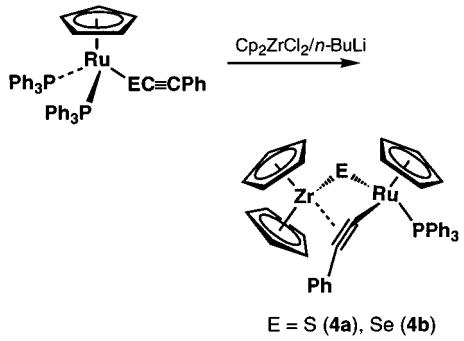

comparable to those of organic alkynes.[15] The S−C1−C2 and Se−C1−C2 spines are nearly linear. The S−C and Se−C distances are similar to those of $Cp_2Ti(SC{\equiv}CPh)_2$ (av. 1.686 Å) and $(C_5H_4Me)_2Ti(SeC{\equiv}CPh)_2$ (av. 1.848 Å),[1] and fall in the normal range of S(Se)−C single bond lengths. These geometric parameters clearly show that the alkynethiolates and alkyneselenolates coordinate at Ru as ordinal thiolate ligands,[1,2,7b,16] and that there is no contribution of the thioketenyl and selenoketenyl resonance forms in their structures as was proposed for $CpRu(PMe_3)_2(\eta^1\text{-}C(Ph){=}C{=}S)$.[7]

Reactions of Ruthenium(II) Alkynechalcogenolato Complexes with Zirconocene(II). It is known that treatment of 2 equiv of *n*-BuLi with Cp_2ZrCl_2 at low temperature produces a highly reactive zirconocene(II) complex via formation of $Cp_2Zr(n\text{-}Bu)_2$ and then $Cp_2Zr(\eta^2\text{-}CH_2{=}CHCH_2CH_3)$.[17] We examined the reaction of $CpRu(PPh_3)_2(SC{\equiv}CPh)$ (**1a**) with Cp_2Zr, which was generated in situ at −78 °C in THF. The consequence was isolation of a hetero-bimetallic complex, $CpRu(PPh_3)(C{\equiv}CPh)(\mu\text{-}S)ZrCp_2$ (**4a**), as red crystals in 70% yield (Scheme 2). During this reaction, one phosphine molecule was liberated from **1a**, and C−S bond cleavage of the alknyethiolato ligand took place, presumably via oxidation of the zirconium atom from II to IV. Thus generated are alkynyl and sulfide moieties bridging the ruthenium and zirconium atoms. A similar C−S bond cleavage was reported to occur in the reaction of $RC{\equiv}CSC_2H_5$ (R = CH_3, Ph) with $Fe_2(CO)_9$, generating $Fe_2(CO)_6(\mu\text{-}SC_2H_5)(\mu\text{-}C{\equiv}CR)$.[18] The reaction of $CpRu(PPh_3)_2(SeC{\equiv}CPh)$ (**2a**) with Cp_2Zr gave rise to an analogous alkynyl−selenido complex $CpRu(PPh_3)(C{\equiv}CPh)(\mu\text{-}Se)ZrCp_2$ (**4b**) as brown crystals in 84% yield. Complexes **4a** and **4b** are air- and moisture-sensitive, but are thermally stable. No decomposition occurred in C_6D_6 at 80 °C for 1 day in the absence of air, as monitored by the ^1H NMR spectra. In each of the ^1H NMR spectra, three Cp signals of equal intensity were observed along with the phenyl proton signals, and thereby, the two Cp rings at Zr are not chemically equivalent. The ^{77}Se NMR spectrum of **4b** consists of a somewhat broad peak at δ 522 and exhibits a substantial low-field shift relative to those of the alkyneselenolato complexes, **2a** and **2b**. The IR spectra of **4a** and **4b** are featured by the C≡C stretching bands appearing at 1926 and 1920 cm^{-1}, which are significantly shifted to lower frequencies compared to those of **1a** and **2a**, as shown in Table 2. Interactions between C≡C π-electrons and a metal center are thus suggested.[19,20] The ^{13}C NMR spectrum of **4a** shows the alkynyl carbon signals at 188.65 ppm (C_α, $^2J_{C-P}$ = 19.6 Hz) and 115.79 ppm (C_β), which are substantially shifted downfield compared with those of **1a**, and the alkynyl carbon signals of the Se-congener (**4b**) appear in a similar region. The situation is similar to the downfield shifts of the ^{13}C NMR signals of $\{(\eta^5\text{-}C_5MeH_4)Zr(\mu\text{-}C{\equiv}CPh)\}_2$ (228.9 ppm, C_α; 154.7 ppm, C_β)[19] and $Cp_2Zr(\mu\text{-}C{\equiv}CSiMe_3)Ni(PPh_3)(\mu\text{-}C{\equiv}CSiMe_3)$ (233.9 ppm, C_α; 112.1 ppm, C_β),[21a] relative to those of $(\eta^5\text{-}C_5MeH_4)_2Zr(C{\equiv}CPh)_2$ (142.8 ppm, C_α; 122.1 ppm, C_β) and $NiCl(C{\equiv}CSiEt_3)(PMe_3)_2$ (121.73 and 121.15 ppm, $C_\alpha$and C_β).[21b]

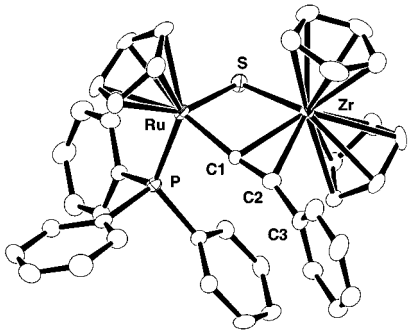

Figure 3. Structure of $CpRu(PPh_3)(C{\equiv}CPh)(\mu\text{-}S)ZrCp_2$ (**4a**) showing 50% probablity ellipsoids.

Table 4. Selected Bond Distances (Å) and Angles (deg) for $CpRu(PPh_3)(C{\equiv}CPh)(\mu\text{-}S)ZrCp_2$ (**4a**), $CpRu(PPh_3)(C{\equiv}CPh)(\mu\text{-}Se)ZrCp_2$ (**4b**), and $CpRu(CO)(C{\equiv}CPh)(\mu\text{-}Se)ZrCp_2$ (**5b**)

	4a	4b	5b
Ru−Zr	3.161(1)	3.219(2)	3.1420(9)
Ru−E	2.414(2)	2.527(2)	2.494(1)
Zr−E	2.444(3)	2.598(2)	2.588(1)
Ru−P	2.285(2)	2.282(4)	
Ru−C1	1.976(8)	1.99(1)	1.959(7)
Zr−C1	2.418(7)	2.43(1)	2.424(7)
Zr−C2	2.550(7)	2.53(1)	2.529(8)
C1−C2 (C≡C)	1.22(1)	1.20(2)	1.22(1)
Ru−C24			1.84(1)
C≡O			1.128(9)
Ru−E−Zr	81.18(7)	77.82(6)	76.35(3)
Ru−C1−Zr	91.4(2)	92.8(4)	91.0(3)
E−Ru−C1	89.5(2)	97.7(3)	103.3(2)
E−Zr−C1	85.0(2)	85.6(3)	88.8(2)
E−Zr−C2	112.0(2)	112.4(4)	117.1(2)
C1−Zr−C2	28.4(3)	27.8(5)	28.4(2)
Ru−C1−C2	173.0(6)	173(1)	170.9(7)
C1−C2−C3	159.7(8)	159(2)	154.9(8)
Ru−C≡O			177.8(9)

The molecular structures of **4a** and **4b** were established by X-ray analysis. The crystals of **4a** and **4b** are isomorphic, and their molecular structures are also very similar. Figure 3 shows the ORTEP view of **4a**, and the selected bond distances and angles of **4a** and **4b** are listed in Table 4. The two metal centers are linked by μ-chalcogenido and μ-σ, π-alkynyl moieties. The alkynyl bridge is unsymmetric in that the terminal carbon of alkynyl is σ-bonded to ruthenium, while zirconium interacts with

(14) Howard, W. A.; Trnka, T. M.; Parkin, G. *Inorg. Chem.* **1995**, *34*, 5900−5909.
(15) March, J. W. *Advanced Organic Chemistry*; Wiley: New York, 1985.
(16) Beswick, M. A.; Raithby, P. R.; Steiner, A.; Vallat, J. C.; Verhorevoort, K. L.; Wright, D. S. *J. Chem. Soc., Dalton Trans.* **1996**, 2183−2184.
(17) Negishi, E.; Holmes, S. J.; Tour, J. M.; Miller, J. A.; Cederbaum, F. E.; Swanson, D. R.; Takahashi, T. *J. Am. Chem. Soc.* **1989**, *111*, 3336−3346.
(18) Rosenberger, C.; Steunou, N.; Jeannin, S.; Jeannin, Y. *J. Organomet. Chem.* **1995**, *494*, 17−35.
(19) Erker, G.; Frömberg, W.; Benn, R.; Mynott, R.; Angermund, K.; Krüger, C. *Organometallics* **1989**, *8*, 911−920.
(20) Akita, M.; Terada, M.; Oyama, S.; Moro-oka, Y. *Organometallics* **1990**, *9*, 816−825.
(21) (a) Rosenthal, U.; Pulst, S.; Arndt, P.; Ohff, A.; Tillack, A.; Baumann, W.; Kempe, R.; Burlakov, V. V. *Organometallics* **1995**, *14*, 2961−2968. (b) Klein, H.-F.; Zwiener, M.; Petermann, A.; Jung, T.; Cordier, G.; Hammerschmitt, B.; Florke, U.; Haupt, H.-J.; Dartiguenave, Y. *Chem. Ber.* **1994**, *127*, 1569−1578.

both alkynyl carbons in a side-on fashion. The Ru−C1 distances are comparable to those found in known Ru(II) alkynyl complexes, e.g., CpRu(C≡CPh)(dppe) (2.009(3) Å)[22] and [Cp*Ru(C≡CTol)(μ-S^{i}Pr)]$_2$ (2.04(3), 2.00(2) Å).[23] The Zr−C2 distances are considerably longer than the Zr−C1 distances, and the phenyl group is bent away from the zirconium side by ca. 20°. The Ru−C1−C2 bonds are approximately linear. These geometric features are often observed for dinuclear complexes with unsymmetrically bridged μ-σ, π-alkynyl ligands.[20,21a,24] Bending of the phenyl group, along with the aforementioned significant shift of $\nu_{C\equiv C}$ values to lower frequencies, indicate Zr−alkyne π-interactions. On the other hand, elongation of the C≡C bonds is not discernible in the X-ray data, and the Zr−C2 distances are very long. Thus Zr−alkyne back-bonding, if any, must be weak. This view is consistent with our assignment of the Zr(IV) oxidation state, as described later, for a d^0 metal center does not back-donate electrons to a π* orbital(s) of alkyne.

The phenyl ring is oriented perpendicular to the RuZrC1C2 plane, as is incarnated by the dihedral angle of 87.5 ° for **4a** and 88.4 ° for **4b**. The RuZrEC1 quadrilateral is puckered by 25.7 ° for **4a** and 25.5 ° for **4b**, and the Ru−E−Zr angles are acute. The Zr−Ru distances of 3.161(1) and 3.219(2) Å are too long to invoke metal−metal bonding.[25] The Ru atom is surrounded by one Cp$^-$, one μ-E$^-$, and one σ-bonded alkynyl$^-$, while the Zr atom is surrounded by two Cp$^-$ ligands, one μ-E$^-$, and one neutral C≡C. From the ligand arrangements in **4a** and **4b**, one may be tempted to consider the formal oxidation states of the metal centers to be Ru(III) and Zr(III). However, the metal−metal separation is large and yet the complexes are diamagnetic, according to the NMR spectra. The related Zr(III)/Zr(III)[19,26] and Zr(III)/Ni(I)[21a] dinuclear complexes were reported to be diamagnetic, while metal−metal distances are long. It was suggested that magnetic coupling via the alkynyl bridging group was responsible for the diamagnetism. We alternatively suggest a zwitterionic form for **4a** and **4b** with Zr(IV)$^+$ and Ru(II)$^-$ centers. In fact, the metal−ligand bond distances fit this interpretation.

A mechanism for the formation of **4a** and **4b** is proposed in Scheme 3. The first step is interaction of the zirconocene(II) center with the alkyne carbons and/or the chalcogen atom of alkynechalcogenolate. This assumption is not labored considering the coordinative unsaturation of zirconocene(II). In close proximity to Zr(II), oxidative addition of the C−S(Se) bonds of alkynechalcogenolates would be promoted to produce a chalcogen-bridged Zr/Ru dinuclear complex (**A**). Then, the alkynyl ligand moves from zirconium to ruthenium, resulting in the formation of **4a** and **4b**.

Scheme 3

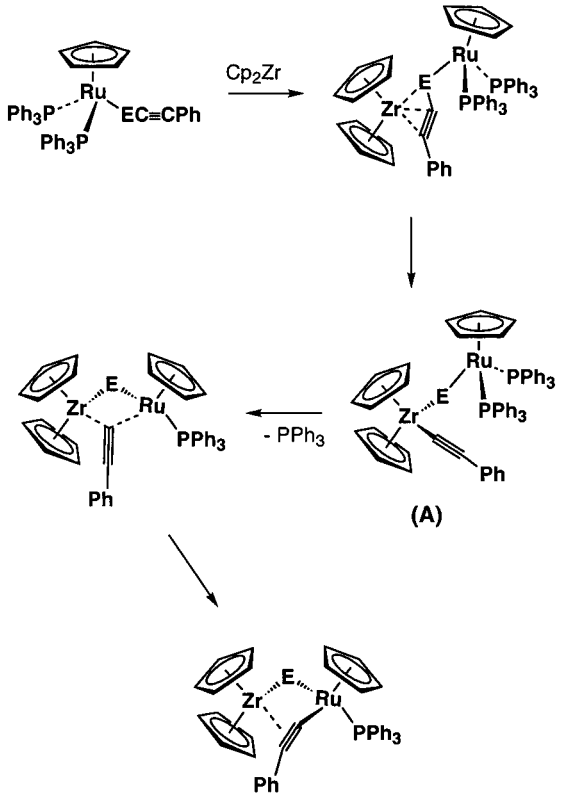

Scheme 4

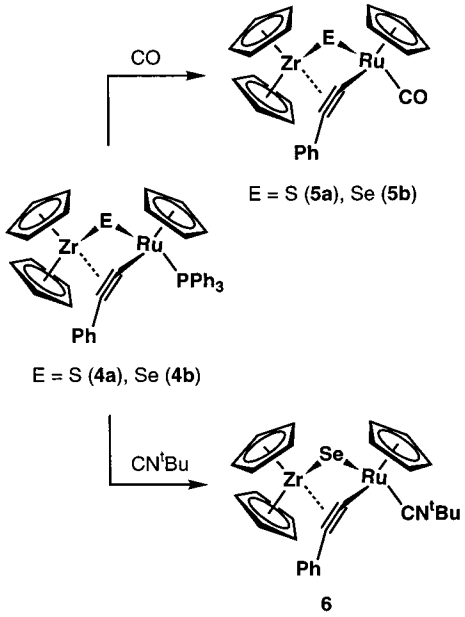

Reactions of the Heterobimetallic Complexes 4a and 4b with CO and ^{t}BuNC. Reactivity of CpRu(PPh$_3$)(C≡CPh)(μ-E)ZrCp$_2$ (E = S (**4a**), Se (**4b**)) was investigated by NMR tube experiments. By monitoring the ^{1}H NMR spectra in C_6D_6, we found that these heterobimetallic complexes reacted cleanly with CO and ^{t}BuNC, liberating the phosphine ligand at Ru. On the other hand, **4a** and **4b** were inert toward 1 atm H_2 and CO_2 and did not react with PhNCO or PhC≡CH either. On a preparative scale, **4a** and **4b** were treated in THF with 1 atm CO at room temperature, and we isolated the carbonyl complexes, CpRu(CO)(C≡CPh)(μ-E)ZrCp$_2$ (E = S (**5a**), Se (**5b**)), as an orange powder in 83% yield and as reddish brown crystals

(22) Bruce, M. I.; Humphrey, H. G.; Snow, M. R.; Tiekink, E. R. T. *J. Organomet. Chem.* **1986**, *314*, 213−225.
(23) Matsuzaka, H.; Hirayama, Y.; Nishio, M.; Mizobe, Y.; Hidai, M. *Organometallics* **1993**, *12*, 36−46.
(24) (a) Ciriano, M.; Howard, J. A. K.; Spencer, J. L.; Stone, G. A.; Wadepohl, H. *J. Chem. Soc., Dalton Trans.* **1979**, 1749−1756. (b) Forniés, J.; Lalinde, E.; Martínez, F.; Moreno, M. T.; Welch, A. J. *J. Organomet. Chem.* **1993**, *455*, 271−281. (c) Janssen, M. D.; Köhler, K.; Herres, M.; Dedieu, A.; Smeets, W. J. J.; Spek, A. L.; Grove, D. M.; Lang, H.; van Koten, G. *J. Am. Chem. Soc.* **1996**, *118*, 4817−4829. (d) Back, S.; Rheinwald, G.; Lang, H. *J. Organomet. Chem.* **2000**, *601*, 93−99.
(25) (a) Casy, C. P.; Jordan, R. F.; Rheingold, A. L. *J. Am. Chem. Soc.* **1983**, *105*, 665−667. (b) Casy, C. P.; Jordan, R. F.; Rheingold, A. L. *Organometallics* **1984**, *3*, 504−506. (c) Gade, L. H.; Schubart, M.; Findeis, B.; Fabre, S.; Bezougli, I.; Lutz, M.; Scowen, I. J.; McPartlin, M. *Inorg. Chem.* **1999**, *38*, 5282−5294. (d) Gade, L. H.; Friedrich, S.; Trösch, D. J. M.; Scowen, I. J.; McPartlin, M. *Inorg. Chem.* **1999**, *38*, 5295−5307.
(26) Lang, H.; Blau, S.; Nuber, B.; Zsolnai, L. *Organometallics* **1995**, *14*, 3216−3223.

in 63% yield, respectively. Analogously, addition of 1 equiv of *tert*-butyl isocyanide to a THF solution of **4b** led to the formation of $CpRu(CN^tBu)(C{\equiv}CPh)(\mu\text{-Se})ZrCp_2$ (**6**), which was isolated as reddish brown crystals in 62% yield (Scheme 4). The ^1H NMR spectra of **5a**, **5b**, and **6** are consistent with their formulation, and there appear three Cp ^1H NMR signals, as in the case of **4a** and **4b**. The strong IR bands at 1965 cm^{-1} for **5a** and 1970 cm^{-1} for **5b** can be assigned to the CO stretching vibrations, and the ^{t}BuNC band of **6** appears at 2120 cm^{-1}. The ^{77}Se NMR signal of **5b** is shifted upfield by 111 ppm compared to that of **4b**, while the C≡C stretching bands in the IR spectra of **5a**, **5b**, and **6** appear in the region similar to those of **4a** and **4b**. These spectroscopic data indicate that the dinuclear structures of **4a** and **4b** are retained when phosphine is replaced by CO or ^{t}BuNC at the Ru site.

The dinuclear structure of **5b** was confirmed by an X-ray crystallographic study, as shown in Figure 4. The selected bond distances and angles are added to the third column of Table 4. The Ru−Se bond length and Ru−Zr distance of **5b** are shortened by 0.077 and 0.033 Å compared with the corresponding distances of **4b**. The large Ru dπ−CO π^* back-donation may have strengthened the Ru−Se bond, which would in turn shorten the Ru−Zr distance. Or, the shortening may be ascribed to the steric factor in that CO is less sterically demanding than PPh_3. The Ru−CO bond is substantially shorter than the Ru−C≡CPh bond, showing that back-donation occurs much more effectively to CO than to the alkynide ligand.[27] The dihedral angle of the ring and the RuZrC1C2 least-squares plane is 12.2°. Thus, the phenyl ring is oriented in such a way that delocalization of electrons may occur between the alkyne portion and the ring. An interesting feature of the dinuclear structure of **5b** is that the ZrRuSe/ZrRuC1 dihedral angle is as small as 7.2°, and therefore, the ZrRuSeC1 quadrilateral core is nearly planar, which is in contrast to the puckered cores of **4a** and **4b**.

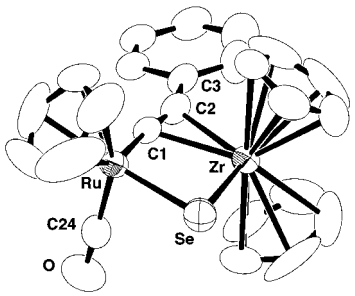

Figure 4. Structure of $CpRu(CO)(C{\equiv}CPh)(\mu\text{-Se})ZrCp_2$ (**5b**) showing 50% probablity ellipsoids.

Supporting Information Available: Eight X-ray crystallographic files in CIF format. This material is available free of charge via the Internet at http//pubs.acs.org.

IC010826H

(27) Kostic, N. M.; Fenske, R. F. *Organometallics* **1982**, *1*, 974−982.